Table III. Comparison of Entropy and Enthalpy Changes of Sm(III) Complexation

ligand	ΔH, kcal/mol	ΔS, cal/(deg mol)	ΔH^c, kcal/mol	ΣZ_2
squarate	+2.00	19.6	+1.25	−1.00
croconate	+0.86	17.1	+0.86	−1.00
kojate	−0.50	25.8	−3.11	−1.67
tropolonate	−2.81	22.2	−4.34	−1.72

polonate has an aromatic ring of six π electrons. However, the cyclic ether rings of the kojate and maltolate ligands are nonaromatic with four π electrons.

Table III compares the enthalpies and entropies of complexation of Sm(III) with croconate and related ligands. The overall complexation reaction can be described in two steps:

$$M(H_2O)_x \rightarrow M(H_2O)_y + (x-y)H_2O \qquad \Delta H_H, \Delta S_H \quad (2a)$$

$$L(H_2O)_n \rightarrow L(H_2O)_m + (n-m)H_2O \quad (2b)$$

$$M(H_2O)_y + L(H_2O)_m \rightarrow ML(H_2O)_{y-m} \quad \Delta H_R, \Delta S_R \quad (3)$$

In general, in lanthanide reactions involving inner-sphere complexation, $\Delta H_H > \Delta H_R$ and $\Delta S_H > \Delta S_R$.[14] Since ΔH_R and ΔS_R should be negative whereas ΔH_H and ΔS_H should be positive, the experimental positive values are in agreement with these relationships. Moreover, there is good evidence for a compensation in these dehydration terms such that $\partial \Delta H_H = T\partial \Delta S_H$.[14,15] If we assume that the differences in the entropies in Table III reflect differences in ΔS_H (since the ligands are all bidentate, we would expect ΔS_R to be very similar), we can correct the enthalpies to constant entropy values such that the differences in the corrected enthalpies, ΔH^c, reflect differences in the ΔH_R terms only. The correction is $\Delta H^c = \Delta H - T\partial \Delta S$, where $\partial \Delta S = \Delta S - 17.1$ cal/(deg mol) (this uses croconate as the base for correction).

The ΔH^c values are listed in Table III. The ΔH^c values have a linear correlation with $\sum Z_2$ which is expected if $\Delta H^c \propto \Delta H_R$ and is related by ligand only to ΔH_R. We ascribe the differences in the experimental ΔH values of complexation for the different ligands primarily to the relationship between the ΔH_R terms and the ligand charge and secondarily to the (smaller) differences due to different dehydration rates.

Acknowledgment. We wish to acknowledge valuable discussions with Professor H. Walborsky in the interpretation of these results. This research was supported by a contract with the U.S. Energy and Development Agency (now DOE).

Registry No. Squaric acid, 2892-51-5; croconic acid, 488-86-8; kojic acid, 501-30-4; tropolone, 533-75-5; maltol, 118-71-8; Ce, 7440-45-1; Pr, 7440-10-0; Nd, 7440-00-8; Sm, 7440-19-9; Eu, 7440-53-1; Gd, 7440-54-2; Tb, 7440-27-9; Dy, 7429-91-6; Ho, 7440-60-0; Tm, 7440-30-4; Yb, 7440-64-4; Lu, 7439-94-3; Y, 7440-65-5; La, 7439-91-0.

References and Notes

(1) E. Orebaugh and G. R. Choppin, *J. Coord. Chem.*, **5**, 123 (1976).
(2) K. Yamada and Y. Hirata, *Bull. Chem. Soc. Jpn.*, **31**, 550 (1958).
(3) A complete description of the mathematical analysis is presented in E. Orebaugh, "Complexation Thermodynamics of Lanthanide Oxocarbon Systems", Ph.D. Dissertation, The Florida State University, 1972.
(4) R. Munze, *J. Inorg. Nucl. Chem.*, **34**, 661 (1972).
(5) G. R. Choppin and R. J. Unrein, "Transplutonium 1975", W. Muller and R. Linder, Ed., North-Holland Publishing Co., Amsterdam, 1976, p 97.
(6) N. K. Dutt and U. V. M. Sharma, *J. Inorg. Nucl. Chem.*, **32**, 1035 (1970).
(7) R. Stampfli and G. R. Choppin, *J. Coord. Chem.*, **1**, 173 (1972).
(8) D. L. Campbell and T. Moeller, *J. Inorg. Nucl. Chem.*, **32**, 945 (1970).
(9) J. D. Roberts, R. Stewart, and M. C. Caserio, "Organic Chemistry", W. A. Benjamin, New York, N.Y., 1971, p 145.
(10) L. W. Schwartz and L. O. Howard, *J. Phys. Chem.*, **74**, 4374 (1970).
(11) R. I. Gelb, L. M. Schwartz, D. A. Laufer, and J. O. Yardley, *J. Phys. Chem.*, **81**, 1268 (1977).
(12) S. S. Yun and G. R. Choppin, *J. Inorg. Nucl. Chem.*, **38**, 332 (1976).
(13) M. H. Palmer, "The Structures and Reactions of Heterocyclic Compounds", St. Martin's Press, New York, N.Y., 1967, p 213.
(14) G. R. Choppin, *Pure Appl. Chem.*, **27**, 23 (1971).
(15) G. R. Choppin, M. P. Goedkin, and T. F. Gritmon, *J. Inorg. Nucl. Chem.*, **39**, 2025 (1977).

Contribution from Ames Laboratory—USDOE and the Department of Chemistry, Iowa State University, Ames, Iowa 50011

Polarized Electronic Absorption Spectra for Potassium Tetrabromoplatinate(II) Dihydrate. Spectral Effects of a Platinum(IV) Component

TIMOTHY J. PETERS, ROY F. KROENING, and D. S. MARTIN, JR.*

Received December 27, 1977

Crystals of the metastable compound $K_2PtBr_4 \cdot 2H_2O$ have an orthorhombic structure, space group *Pbam*, with *a*:*b*:*c* = 8.31 (2):13.73 (3):4.84 (1) Å and $Z = 2$. The $PtBr_4^{2-}$ ion occupies a crystallographic site of C_{2h} symmetry but retains essentially a D_{4h} molecular symmetry with the *z* axis directed along *c*. The absorption spectra in the d ← d region were recorded for *a*, *b*, and *c* polarizations. Band maxima lie at 300–800 cm^{-1} higher energies than in anhydrous K_2PtBr_4. The $^1A_{2g} \leftarrow {}^1A_{1g}$ transition, forbidden in *z* polarization, was not observed in *c* polarization. Vibrational components were resolved in the $^3B_{1g}$ shoulder and in the $^1A_{2g}$ peak. Striking differences in intensities which occurred in the *a* and *b* polarization indicated that crystal effects were important in the vibronic excitation process. Red sections, in some crystals, were attributed to a dipole-allowed band, completely *c* polarized, for a mixed-valence electron-transfer transition involving a $PtBr_6^{2-}$ impurity defect.

Introduction

When a solution of potassium tetrabromoplatinate(II) evaporates at room temperature, some crystals of anhydrous K_2PtBr_4 are formed. The structure, determined by X-ray diffraction, and polarized crystal absorption spectra of these crystals were described previously.[1] However, the formation of a hydrate can also occur. This hydrate, characterized as $K_2PtBr_4 \cdot 2H_2O$, was described by Biilman and Anderson[2] as black crystals which were very rapidly dehydrated when exposed to laboratory air. However, they reported angles between well-developed faces of these crystals and concluded that they were orthorhombic.

In anhydrous K_2PtBr_4 the square-planar $PtBr_4^{2-}$ occupies a site of full D_{4h} symmetry, and the polarized crystal spectra

0020-1669/78/1317-2302$01.00/0

have provided the molecular polarizations of the transitions which have assisted assignment of the d–d and some charge-transfer transitions. The present studies were undertaken to obtain the effects of a different crystal environment for the $PtBr_4^{2-}$ ion in a site of lower symmetry upon the energies and the intensities of the electronic transitions.

Experimental Section

The preparation of K_2PtBr_4 has been described earlier.[1] Solutions of K_2PtBr_4 were subject to a slow disproportionation reaction. Over extended periods, some precipitation of metal was observed and presumably $PtBr_6^{2-}$ formed in the solution.

We were attempting to prepare thin crystals of K_2PtBr_4 for spectroscopy by evaporating solutions of K_2PtBr_4 between microscope slides. It was noted that large crystals (several mm^2 in area) of the hydrated crystals frequently formed. Most commonly, the observed face of the exceedingly thin crystals formed by this technique was rectangular and distinctly dichroic with a pale pink color for an extinction with polarization in the direction of the long crystal dimension and a tan color for the other extinction direction. Occasionally, triangular faces were obtained with tan color for both polarizations but with distinctly different absorption intensities.

The life of the $K_2PtBr_4 \cdot 2H_2O$ crystals, when exposed to air, was exceedingly short. When microscope slides with crystals and solution were separated, the dehydration transformation was complete, and the crystals were opaque before they could be lifted from the slides. Also, all attempts to introduce a crystal into a glass capillary for X-ray diffraction proved unsuccessful. On some occasions when the slides remained together for several weeks, a large single hydrate crystal was observed to transform into several transparent anhydrous crystals with random orientation of axes and with gaps between them. However, it was necessary to utilize techniques which did not require the separation of crystals from the mother liquor for both the X-ray diffraction and the spectroscopic studies.

Crystal Structure Determination. The crystal for X-ray diffraction was obtained by inserting a small droplet of the saturated K_2PtBr_4 solution into a drop of methylcellulose solution (clear fingernail polish). The methylcellulose was placed on a polyethylene sheet, and it could be cut away from the polyethylene after it hardened. In many of the vacuoles prepared, multiple crystals were observed to form as apparently water diffused from the solution into the methylcellulose. In cases where single crystals were thought to form, the hardened droplets were cemented to a glass fiber for mounting on the goniometer head of an automatic four-circle X-ray diffraction unit. In all, about 20 crystals were mounted for diffraction. A large number of twinned crystals were obtained, and several anhydrous K_2PtBr_4 crystals were indexed before a crystal was found which was indexed with an orthorhombic unit cell. This crystal, measured under a microscope with a calibrated scale, was found to be $0.40 \times 0.36 \times 0.04$ mm^3.

X-ray intensity data were collected with a Mo Kα (0.7107 Å) radiation source, which was used with a graphite monochromator, by means of a scintillation counter on the four-circle diffractometer. The data were collected for the hkl and $hk\bar{l}$ octants within a 2θ region of 50°. Three standard noncoplanar reflections were chosen to monitor changes in the intensity, and the intensities of all of the standard reflections showed very considerable and different increases during the collection period. This increase in intensity was believed to be due to an increase in mosaic character of the crystal during the period. A total of 1200 reflection counts were recorded by the step-scan technique.[3] These reflections constituted nearly two complete octants of data; however, before further data could be collected, the specimen abruptly lost its crystallinity and ceased to diffract. The growth of intensity for the standard reflections appeared to be linear with respect to time (reflection number), and the rates of increases were taken from the least-squares slopes of three intensities of the three standard reflections. The increase was apportioned from the three standards to the **a***, **b***, **c*** vectors, and an intensity correction for each point was taken proportional to its h, k, l values. Equivalent reflections from the different octants were averaged and 65 reflections were eliminated for which the deviations of the individual F values from the average were greater than 30%. Thus, a total of 470 unique reflections were utilized for the structure determination.

Single-Crystal Spectroscopy. Crystals for spectroscopy were grown by the evaporation of a film of solution between fused-quartz plates, $12 \times 19 \times 1.6$ mm^3. Frequently, crystals sufficiently large would grow near the center of the plates so that a pinhole, approximately 1 mm in diameter, in a metal sheet could be cemented over one of the plates to confine the beam completely to the crystal. Such crystals might survive for several days at room temperature. The quartz plates with the pinhole, still containing the mother liquor in contact with the crystal, were clamped into the copper tail of a cryostat mounted over the sample compartment of the spectrophotometer. This copper tail served as the bottom of the container for the cryogenic fluid. The cryostat was quickly pumped down with a mechanical pump, and liquid nitrogen was added to the outer and inner chambers of the cryostat as soon as a rough vacuum was obtained. The mother liquor between the plates would freeze, and the vapor pressure of the hydrate crystals was lowered by the cooling so crystals could survive for the recording of their spectra at liquid-nitrogen temperature and also when the nitrogen in the inner chamber was replaced by liquid helium. Since cooling of the specimen was by conduction through the fused-quartz plates, an upper limit on the crystal is placed rather conservatively, it is believed, at 15 K. The thickness of one crystal was determined from the separation of the interference peaks resulting from the multiple reflections between the quartz plates at several positions in the air gap around the crystal. The thickness of other crystals was evaluated by a comparison of the height of peaks in their spectra with the height of peaks of this standard crystal. The instrumentation utilized to measure the absorption spectra of single crystals has been described previously.[4] It was apparent that freezing of the solution film between the fused-quartz plates sometimes separated the plates from the crystal, and serious interference effects were introduced into the spectra. However, very satisfactory spectra were recorded in a reasonable fraction of the experiments so that the features reported here have been reproduced several times with different crystals.

Results and Discussion

Crystal Structure of $K_2PtBr_4 \cdot 2H_2O$. The crystals of $K_2PtBr_4 \cdot 2H_2O$ were found to have orthorhombic unit cell parameters of $a:b:c$ = 8.31 (2):13.73 (3):4.84 (1) Å, V = 552 Å^3, and Z = 2. The observed extinction conditions were consistent with either of the space groups *Pba*2 or *Pbam*. These two groups differ only in that *Pbam* possesses an inversion center whereas *Pba*2 does not. A Howells–Phillips–Rodgers (HPR) plot[5] was inconclusive in indicating the presence or absence of an inversion center. The data, therefore, were refined under both space groups; since no significant difference in the level of refinement was obtained, the results are reported for *Pbam*.

A three-dimensional Patterson map was constructed from the reflection data, and preliminary atom positions were determined from this map. With the platinum atom at the origin, the two unique Br positions and one K and one O were introduced, and the structure was refined using a full-matrix least-squares procedure in a local modification of ORFLS.[6] Scattering factors of Doyle and Turner[7] were used. Absorption in the crystal should have been significant. Such corrections were attemptd by the two different programs ORABS[8] and TALABS.[9] In each case the data with absorption conditions did not refine as well as the uncorrected data. Despite the limitations in the data, the conventional discrepancy factor R, $R = \sum||F_o| - |F_c||/\sum|F_o|$, reduced to a value of 0.18.[10] The atomic positions indicated in the structure are included in Table I, and a unit cell is shown in Figure 1. The oxygen position did not settle out, and its positional coordinates have a high uncertainty. However, the positions shown are centered in the only holes in the packing of Pt, Br, and K atoms sufficiently large to contain the water molecule. Although temperature factors, restricted by the symmetry conditions, were included in the refinement, they have not been reported in view of the uncertainty in the data.

From the data in Table I it is apparent that the $PtBr_4^{2-}$ has, within reasonable experimental uncertainty, retained its molecular D_{4h} symmetry in the hydrate, and the Pt–Br distances of 2.446 (6) and 2.43 (1) Å agree well with the 2.445 (2) Å for K_2PtBr_4.[1] The ions stack in the hydrate with a separation of 4.84 Å, some 0.52 Å greater than in the K_2PtBr_4.

Table I. Atomic Positions and Interatomic Distances and Angles for $K_2PtBr_4 \cdot 2H_2O$

atom	x	y	z
Pt	0	0	0
Br_1	0.291 (1)	0.0266 (6)	0
Br_2	−0.041 (1)	0.1754 (6)	0
K	0.255 (3)	0.193 (2)	0.5000
O	0.12 (9)	0.360 (6)	0.5000

Distances, Å

Pt-Br_1	2.446 (6)	Br_2''-K[a]	3.46 (2)
Pt-Br_2	2.43 (1)	Br_1-Br_1'[b]	3.550 (9)
Br_1-Br_2	3.430 (1)	Br_1-Br_2''	4.33 (1)
Br_1-K	3.340 (2)	Br_2-Br_2''	4.63 (1)
Br_2-K	3.459 (9)		

Angles, Deg

Br_1-Pt-Br_2 89.4 (1)

[a] The Br'' atoms are on the molecule at $^1/_2,^1/_2,0$. [b] The Br' atoms are on the molecule at 1,0,0.

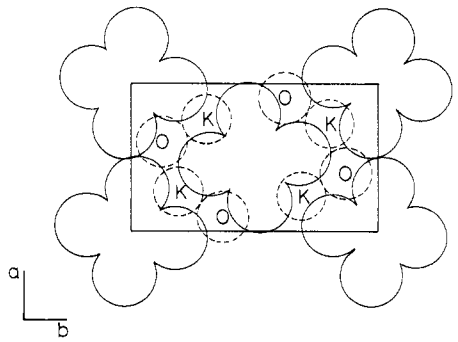

Figure 1. Crystal structure for $K_2PtBr_4 \cdot 2H_2O$. Projection on the 001 face. The $PtBr_4^{2-}$ ions are shown in space filling sections at $z = 0$, and the K^+ and O atoms of H_2O are at $z = 1/2$.

Although the $PtBr_4^{2-}$ ions in the anhydrous compound pack in the 001 plane with the rather inefficient square arrangement, they pack with very nearly a hexagonal array in $K_2PtBr_4 \cdot 2H_2O$. The acute angle between the 110 and the $1\bar{1}0$ faces is 62.4°. The molecular volume accordingly is 276 Å^3 compared to 234 Å^3 for K_2PtBr_4 which provides a difference of 21 Å^3 for each H_2O molecule.

In anhydrous K_2PtBr_4 the potassium ions possess approximately cubic coordination with eight bromide atoms at equal distances. In $K_2PtBr_4 \cdot 2H_2O$ the potassium ion has a trigonal-prismatic coordination of six bromides where the distances range from 3.34 to 3.46 Å and bracket the 3.385 Å distnce in K_2PtBr_4. However, two of the three prismatic faces have been opened up to permit coordination to each of two H_2O oxygens for a total coordination again of eight.

One interesting feature is the close contact of the $PtBr_4^{2-}$ ions along the *a* axis. The Br–Br distance between these ions is only 3.55 Å, scarcely 0.1 Å greater than between bromides in the same ion. This distance is slightly less than twice the normal van der Waals radius[11] of bromine, and the ions must very definitely be in contact along this axis. In contrast, the Br–Br distances between the molecules at the corner and the center of the *c* face are 0.8 and 1.1 Å larger. Thus, there are chains of anions in contact with their neighbors along the *a* axis with the adjacent chains separated by K^+ ions and H_2O molecules. In contrast, each Br in the anhydrous salt has two bromides from different ions at 3.89 Å, some 0.3 Å greater than the short distance in $K_2PtBr_4 \cdot 2H_2O$.

Crystal Spectra of $K_2PtBr_4 \cdot 2H_2O$. In the crystals of this compound the $PtBr_4^{2-}$ ion occupies a site with C_{2h} point symmetry. The *z* molecular axis is aligned along the *c* crystallographic axis, and for an *hk*0 face the *c*-polarized spectrum will give directly the molecular *z* absorption. Since there are two molecules in a unit cell related by symmetry, there will be two Davydov crystal states for each molecular transition. Because of the alignment of the transition dipoles, however, a transition to one of the Davydov states will be forbidden and intensity will only appear in the transition to the other state.

For a 001 face, spectra can be recorded for *a* and *b* polarizations. The *z*-polarized transitions should not be seen in these directions. The transitions seen for this face must arise from molecular *x* and *y* polarizations of two transitions which are degenerate in the D_{4h} molecular symmetry. The C_{2h} site symmetry can split the degeneracy so that *x* and *y* transitions can have different energies. The *x* and *y* excited states will each provide two Davydov states, i.e., four states in all.

Two Davydov transitions, one from *x* and the other from *y* polarization, may be allowed in *a* but forbidden in *b* polarization. The other pair of states will be forbidden in *a* and allowed in *b* polarization. Hence, in general, two transitions, separated by crystal field splittings, may be seen in each polarization. However, the pair of transitions in *a* polarization may be at different energies than the transition in *b* because of Davydov splitting. In addition, intensities in the *a* and *b* polarization may be different. In case crystal effects are negligible and the system can be considered as oriented, noninteracting D_{4h} ions, only a single absorption at the same energy, because of the degeneracy, and with identical intensities would be seen for the *a* and *b* polarizations.

When crystals were grown by evaporation of a freshly prepared saturated solution between fused-quartz plates, the majority of the crystals were needles which had a pale pink color over light polarized along the long direction and a tan color for light polarized perpendicular to the long axis. It was observed that for crystals grown from older solutions sections under the parallel polarization were bright red. The red sections would be adjacent to normal pink sections and would be more extensive the older the solution. Simultaneously, the crystals had an absolutely uniform tan color in the perpendicular polarizations. It is considered that the pale pink sections correspond to pure $K_2PtBr_4 \cdot 2H_2O$, and the red sections are due to an impurity defect which will be discussed below. Since anhydrous K_2PtBr_4 crystals were pink under *c*–*z* polarization and tan under *a*–*x*,*y* polarization, it was concluded that the long dimension of these crystals was along the *c* axis, which, as expected, is the shortest of the three orthorhombic axes.

Less frequently, crystal faces developed which were tan under polarized light along both extinction directions. Frequently, but not always, these faces had sections which were nearly equilateral triangles. The evidence discussed below indicates that these were 001 faces which would have extinction directions along the *a* and *b* crystal axes. However, the absorption was clearly of different intensity along the two extinction polarizations. A crystal was observed for this face as a broad needle with the higher absorption along the long axis of the needle. This needle with very well defined edges had a blunt point on one end. The angles between each needle edge and the adjacent edge which formed the point, were observed to be 121.3 and 121.5° which was in very good agreement with the calculated angle of 121.2° between the 010 face and the 110 face. On the basis of these observations the long dimension of the needle was assigned as the *a* axis which was the extinction direction of the higher absorption. This assignment would correspond to faster growth along the shorter *a* rather than the *b* axis.

Absorption spectra for polarizations along *a*, *b*, and *c* in the region of the d–d transitions are shown for 300 and 15 K in Figure 2. The wavenumber, $\bar{\nu}$, for the maximum of each resolved band together with the molar absorptivity, ϵ_{max}, and the oscillator strengths for the 15 K spectra are included in

Table II. Energy of Band Maxima, Molar Absorptivities, and Oscillator Strengths for $K_2PtBr_4 \cdot 2H_2O$ and for K_2PtBr_4 at 15 K

$K_2PtBr_4 \cdot 2H_2O$										K_2PtBr_4[a]					
a polarization			*b* polarization			*c* polarization			excited state D_{4h} orbital assign	*a* polarization			*c* polarization		
$\bar{\nu}$, cm^{-1}	ϵ_{max}, cm^{-1} M^{-1}	$10^4 f$	$\bar{\nu}$, cm^{-1}	ϵ_{max}, cm^{-1} M^{-1}	$10^4 f$	$\bar{\nu}$, cm^{-1}	ϵ_{max}, cm^{-1} M^{-1}	$10^4 f$		$\bar{\nu}$, cm^{-1}	ϵ_{max}, cm^{-1} M^{-1}	$10^4 f$	$\bar{\nu}$, cm^{-1}	ϵ_{max}, cm^{-1} M^{-1}	$10^4 f$
19600	23	2	19400	22	2	18400	5	0.2	$^3A_{2g}$: $b_{1g}(d_{x^2-y^2}) \leftarrow b_{2g}(d_{xy})$	19100[b]	15	1.7	18800	11	1.1
									^3E_g: $b_{1g}(d_{x^2-y^2}) \leftarrow e_g(d_{xz,yz})$						
23100	20	1.2	23000	20	1.5	23100	2	0.09	$^3B_{1g}$: $b_{1g}(d_{x^2-y^2}) \leftarrow a_{1g}(d_{z^2})$	22700	13	0.9	22600	3	0.2
24700	122	8.5	24700	77	5.9		absent		$^1A_{2g}$: $b_{1g}(d_{x^2-y^2}) \leftarrow b_{2g}(d_{xy})$	24400	46	3.5		absent	
27500	136	12.1	27500	82	8.4	28200	22	1.8	^1E_g: $b_{1g}(d_{x^2-y^2}) \leftarrow e_g(d_{xz,yz})$	26800	73	7.0	27400	44	4.2

[a] From ref 1. [b] For anhydrous K_2PtBr_4 a shoulder was resolved at ca. 17000 cm^{-1}.

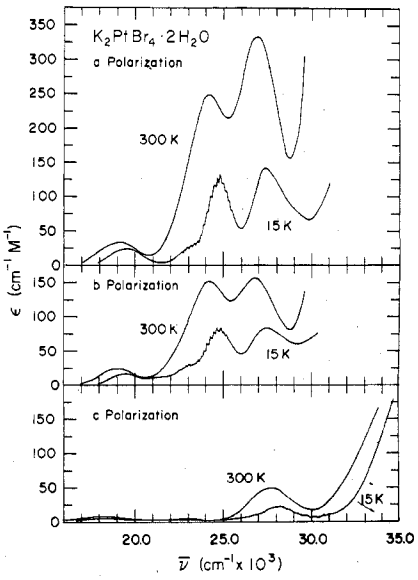

Figure 2. Polarized crystal spectra for $K_2PtBr_4 \cdot 2H_2O$.

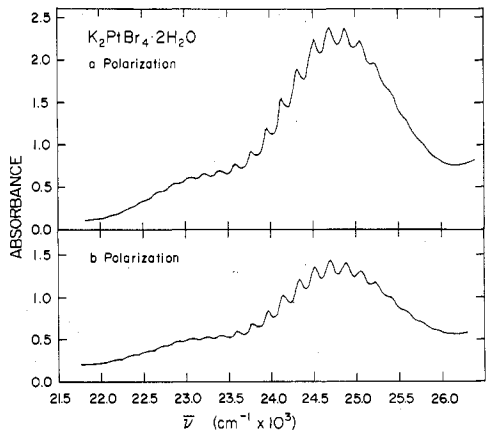

Figure 3. Vibrational structure in the $^3B_{1g}$ and the $^1A_{2g}$ bands of $K_2PtBr_4 \cdot 2H_2O$.

Table III. Vibrational Components Observed at 15 K for $K_2PtBr_4 \cdot 2H_2O$ ($\bar{\nu}$, cm^{-1})

a polarization		*b* polarization		*c* polarization	
22300	24140	22330	24140	22180	22550
22480	24330	22510	24330	22350	22750
22660	24510	22710	24520		
22850	24690	22890	24690		
23030	24880	23060	24880		
23220	25050	23260	25050		
23400	25220	23410	25240		
23580	25390	23590	25420		
23760	25580	23780	25590		
23950		23970			

Table II. The oscillator strengths were calculated from the expression $f = 4.32 \times 10^{-9} \int \epsilon \, d\bar{\nu}$. For comparison, similar data for anhydrous K_2PtBr_4 are included. The qualitative features of the spectra between the two compounds are so similar in the d–d region that the transition assignments for the hydrate follow directly from the earlier assignments of anhydrous K_2PtBr_4. For example, corresponding transition maxima for $K_2PtBr_4 \cdot 2H_2O$ lie from 300 to 800 cm^{-1} higher than the corresponding maxima in K_2PtBr_4. This difference is only slightly larger than the uncertainty in the rather broad peaks. Thus, the weak peak seen from 19400 to 19600 cm^{-1} in *a*, *b*, and *c* polarizations can be assigned to the spin-forbidden transitions $^3A_{2g}$, $^3E_g \leftarrow {}^1A_{1g}$. In the anhydrous crystal a shoulder on this band was seen at 17000 cm^{-1}, but for the hydrates sufficiently thick crystals to demonstrate this shoulder conclusively were not available. The shoulders at 23000–23100 cm^{-1} in *a* and *b* polarization and the weak feature in *c* polarization at this energy can be assigned as the $^3B_{1g} \leftarrow {}^1A_{1g}$ transitions. The $^1A_{2g} \leftarrow {}^1A_{1g}$ transition is vibronically forbidden in *z* molecular polarization; the band seen at 24700 cm^{-1} in *a* and *b* polarization, but absent in *c* polarization, can therefore be assigned to this transition. The highest energy band observed, 27500–28200 cm^{-1}, in all three polarizations is likely the $^1E_g \leftarrow {}^1A_{1g}$ transition.

The small blue shift of 300–800 cm^{-1} in the d–d bands can be rationalized from the packing of the close neighbors about a $PtBr_4^{2-}$ ion. In these transitions an electron is excited from largely a metal orbital into an antibonding metal–ligand orbital so there is some expansion of the electron cloud. For K_2PtBr_4 there are eight K^+ ions equidistant from each Pt at 4.26 Å. For $K_2PtBr_4 \cdot 2H_2O$ there are four K^+ ions at 4.17 Å, but the second four are 5.24 Å away. This arrangement corresponds to a net movement of positive charge away from the center of the $PtBr_4^{2-}$ ion in the hydrate, although the K–Br distances in K_2PtBr_4, which are 3.385 Å, are hardly different from the 3.43-, 3.34-, and 3.46-Å distances in $K_2PtBr_4 \cdot 2H_2O$. Moreover, the very close approach of 3.55 Å for a neighboring bromide ligand, which doubtless bears some negative charge, to each of two bromide ligands of the anions in $K_2PtBr_4 \cdot 2H_2O$ corresponds to a movement of negative charge toward $PtBr_4^{2-}$. Thus, the blue shifts of the d–d bands for $K_2PtBr_4 \cdot 2H_2O$, although small, are consistent with the movement of positive and negative charges about the $PtBr_4^{2-}$ ion and their interactions with the expanding electron density.

The intensities of transitions decrease very significantly upon cooling the crystals from room temperature to 15 K, a characteristic of vibronically excited transitions. In addition, the maxima of the bands are shifted to higher energies by approximately 500 cm^{-1} upon the cooling.

The $^1A_{2g} \leftarrow {}^1A_{1g}$ peaks and the $^3B_{1g} \leftarrow {}^1A_{2g}$ shoulders exhibit resolved vibrational structure in *a* and *b* polarization. These portions of the spectra are shown on an expanded scale in Figure 3, where it can be seen that some 21 components can be discerned. A few ill-defined components in *c* polarization could also be seen in the region of 22180–22750 cm^{-1}

for the $^3B_{1g}$ band. Values of the vibrational components, taken directly from the recorder chart, are presented in Table III. It can be seen from this table that possibly the vibrational components in *b* polarization fall 30–50 cm^{-1} higher than the adjacent component in *a* polarization up to 23 300 cm^{-1}. However, the components are not at all well developed in this region. From 23 300 to 25 200 cm^{-1} with the well-defined peaks in the $^1A_{2g}$ band, the peaks in *a* and *b* polarization fall together within the experimental uncertainty of ±10–20 cm^{-1}. Such a vibrational progression in the bands can be attributed to transitions to excited states of totally symmetric vibrations in the excited electronic states. The square-planar $PtBr_4^{2-}$ ion with D_{4h} symmetry possesses only one A_{1g} vibration, a metal–bromide stretching mode, the breathing vibration. However, under the C_{2h} site symmetry there would be two totally symmetric normal stretching modes. The fact that such a well-defined single progression occurs indicates that the reduction in symmetry has not introduced a symmetric stretching vibration with a significantly different frequency. Also, the intensity for the transition is gained primarily from the vibronic perturbation of a single asymmetric vibration although there are two E_u molecular vibrations which can excite this transition. In addition, the close agreement in the energies of the vibrational peaks which can be measured accurately under the *a* and *b* polarizations give no indication of a breaking of the degeneracy by the crystal field or of a splitting of the Davydov states. The average separation in the progressions across the $^1A_{2g}$ band was 182 cm^{-1}. As would be expected, this value is substantially lower than the $\bar{\nu}_1$ mode for the ground state of $PtBr_4^{2-}$ which was reported by Hendra[12] to be 205 cm^{-1} from the Raman spectrum of K_2PtBr_4. In anhydrous K_2PtBr_4 the separations were only 174 cm^{-1}. This difference between the two frequencies was quite real; for over a fixed wavenumber interval spanning the region of the vibrational structure, the anhydrous crystal would have an additional member in the progression.

Apparently, the packing around the $PtBr_4^{2-}$ ion in the hydrate is such that for the excited $^1A_{2g}$ electronic state, the interactions with the neighbors give a significant increase to the breathing frequency. In K_2PtBr_4, each bromide ligand is in contact with four potassium ions and upon a Pt–Br stretch moves toward the center of a square between the potassiums. However, in $K_2PtBr_4 \cdot 2H_2O$ the Br_1's in a stretching mode move directly toward another bromide with which they are in rather close contact whereas the Br_2's move not exactly but approximately toward a line that connects two potassiums, one above and below the anion. This difference apparently leads to the measurable difference in the observed vibrational frequency for the excited $^1A_{2g}$ state.

Other interesting differences between the anhydrous and hydrated salts involve the resolutions of bands and intensities which involve the vibronic perturbations. The most obvious feature is the difference in intensities in the *a* and *b* polarizations, which quantitatively is represented by molar absorptivities in *a* polarization which are nearly a factor of 2 higher than those of *b* polarization. Since an oriented isolated ion would have equal intensity for any in-plane polarization, the crystal perturbations apparently have quite a profound influence upon the intensities. Indeed, such a difference places in serious question the value of calculated polarization ratios from the orientation of molecular transition dipole moment vectors in situations where the molecular symmetry has been compromised by a lower site symmetry. In $K_2PtBr_4 \cdot 2H_2O$ this large difference in intensity may be the consequence of the close proximity of bromides from different ions along the *a* axis. Thus, lattice motions in the *a* direction may be more effectively translated into intramolecular displacements and give stronger interactions between the lattice and the molecular

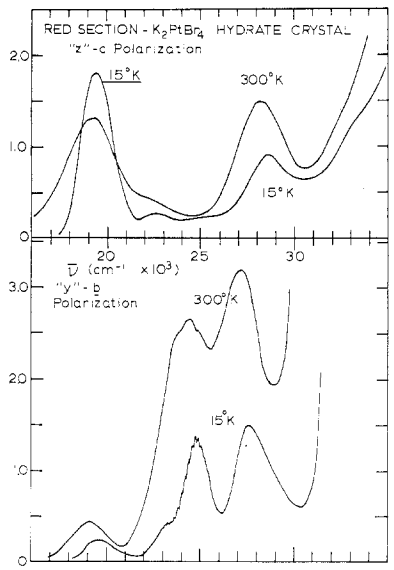

Figure 4. Spectra for a red section for the 100 face of $K_2PtBr_4 \cdot 2H_2O$.

vibrations and consequently larger vibronic perturbations. From a comparison of the ϵ_{max} for the various absorption bands, it appears that the *c*–*z* polarization for the hydrate was of significantly lower intensity than the corresponding bands in the anhydrous compounds. The ^1E_g band in *b* polarization of the hydrate had comparable intensity with that band in the anhydrous *a* polarization. However, other *b*-polarization bands of the hydrate were somewhat more intense than the corresponding bands in K_2PtBr_4. Further, all *a*-polarization bands in the hydrate were considerably stronger than the in-plane polarized bands of the anhydrous crystals.

Another immediately apparent difference was the much better resolution of the $^1A_{2g}$ and ^1E_g bands at room temperature for $K_2PtBr_4 \cdot 2H_2O$. The separation of these transitions was 2800 cm^{-1} at 15 K in the hydrate, only 400 cm^{-1} greater than for the anhydrous crystal. But at 300 K these bands formed clearly two well-resolved peaks in both *a* and *b* polarizations for $K_2PtBr_4 \cdot 2H_2O$ whereas the $^1A_{2g}$ band for K_2PtBr_4 was seen as only a poorly resolved shoulder on the ^1E_g peak. A comment can now be made on the assignment of the 001 face. A general *hkl* face, $l \neq 0$, would contain components of molecular *x*, *y*, and *z* polarizations for both extinction directions and both would exhibit a tan color. Since there is no peak at *z* polarization at 24 700 cm^{-1}, this peak would be of especially low intensity for the extinction direction which had the strongest *z* component. However, this would also be the polarization in which the intensity of the 27 500-cm^{-1} peak would be lower. It can be seen that for the assigned *b* polarization where the intensities are lower, the ratio of the intensities, $^1A_{2g}$:^1E_g, is actually greater than for the *a* polarization. Hence, it is concluded that this is likely the 001 face.

Spectra for the Red Sections. The spectra obtained for a red section of a crystal are shown in Figure 4. Frequently, the red sections would be surrounded by sections with the normal pale pink color for *c*-polarized light. For the *c* polarization in Figure 4 the normal vibronic ^1E_g band can be seen. The red color is a consequence of the somewhat more intense peak at ca. 19 000 cm^{-1}. When the crystal was cooled to 15 K, this band increased in height as it narrowed, a typical characteristic of a dipole-allowed transition in contrast to vibronic transitions. In the *b* polarization of the same crystal, a completely normal absorption was observed and indeed with this polarization no inhomogeneity could be discerned for this *b* polarization. This phenomenon was strikingly similar to the formation of red sections in Cossa's salt, $KPt(NH_3)Cl_3 \cdot H_2O$,

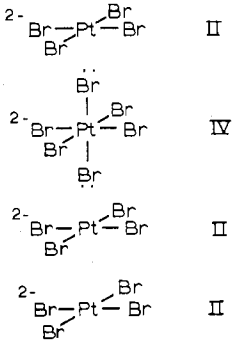

Figure 5. Inclusion of $PtBr_6^{2-}$ as an impurity defect in the stacks of $PtBr_4^{2-}$.

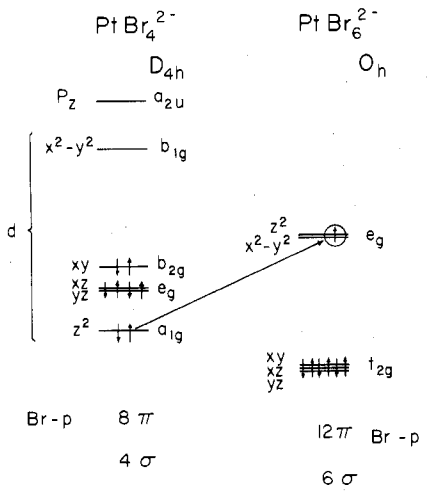

Figure 6. Orbital energy diagram to illustrate the electron transfer from $PtBr_4^{2-}$ to $PtBr_6^{2-}$ in red sections.

where rather good evidence was found to indicate that similar red sections were due to the inclusion of the platinum(IV) ions $Pt(NH_3)Cl_5^-$ in the stacks of $Pt(NH_3)Cl_3^-$ ions.[13] The fact that aging of the crystallizing solutions increased the incidence of red sections was consistent with the inclusion of $PtBr_6^{2-}$ ions in the present case as illustrated in Figure 5. These ions could form by either slow air oxidation or autooxidation–reduction of the $PtBr_4^{2-}$ ion. If a $PtBr_6^{2-}$ ion replaces $PtBr_4^{2-}$ in a lattice site, the axial Br ligand is forced very close to the Pt^{II} atom in the square-planar ion. The $PtBr_4^{2-}$–$PtBr_4^{2-}$ stacking distance in the crystal is just the length of the c axis, 4.84 Å. If one subtracts the normal Pt–Br distance[14] of 2.44 Å from 4.84 Å, this would require that the Br atom approach to within 2.40 Å of the Pt^{II} atom. Presumably, there must be some distortion of the cell to accommodate $PtBr_6^{2-}$. Perhaps, the extent of this distortion precludes the formation of the 1:1 mixed-valence compound, which was observed to form from Cossa's salt but was not observed in the present case. Also, it may explain the absence of such defects in anhydrous K_2PtBr_4 with a c axis of only 4.36 Å. The band at 19 400 cm^{-1} in the red sections can then be assigned as a mixed-valence Pt^{IV} $d_{z^2} \leftarrow Pt^{II}$ d_{z^2} electron transfer as shown in Figure 6. This transition, a $\sigma \leftarrow \sigma$ type, would be polarized in the z–c direction. It does involve the electron transfer through the bromide ligand and requires a very close approach of the bromide to the square-planar Pt^{II} atom. However, such a transfer should be enhanced in that the e_g orbitals of $PtBr_6^{2-}$ are, in fact, antibonding orbitals which include a contribution from the ligand $p(\sigma)$ orbitals. The transition which occurs must be quite intense. $PtBr_6^{2-}$ in aqueous solution has a molar absorptivity[15] of 10 000 cm^{-1} M^{-1} at 30 000 cm^{-1}. From the spectra in Figure 4 a conservative upper limit of about 0.2 mol % can be placed on the $PtBr_6^{2-}$ content from its possible contribution at 30 000 cm^{-1}. Such a defect concentration places a lower limit of 28 000 (cm^{-1} M^{-1} defects) upon its molar absorptivity.

From the indicated orbital energies shown in Figure 6 the electron transfer from the d_{xy} and the $d_{xz,yz}$ orbitals of Pt^{II} into the octahedral e_g orbitals should be energetically possible. An electron transfer from d_{xy} would be either $\sigma \leftarrow \delta$ or $\delta \leftarrow \delta$ and hence dipole-forbidden. A transfer from d_{xz}, d_{yz} would be $\sigma \leftarrow \pi$ or $\delta \leftarrow \pi$ and dipole-allowed in x, y polarization. It appears that the $\sigma \leftarrow \pi$ participation of the bromide orbitals does not give sufficient intensity for this transition to be detected.

Acknowledgment. This study was supported by the U.S. Department of Energy, Office of Basic Energy Sciences, and the Iowa State University Energy and Mineral Resources Research Institute. We are indebted to Professor Robert A. Jacobson for his assistance and advice in the crystal structure determination.

Registry No. $K_2PtBr_4 \cdot 2H_2O$, 65531-65-9.

Supplementary Material Available: A listing of structure factor amplitudes (1 page). Ordering information is given on any current masthead page.

References and Notes

(1) R. F. Kroening, Rhonda M. Rush, Don S. Martin, and J. C. Clardy, *Inorg. Chem.*, **13**, 1366 (1974).
(2) E. Biilman and A. C. Anderson, *Ber. Dtsch. Chem. Ges.*, **36**, 1565 (1903).
(3) L. E. Alexander and G. S. Smith, *Acta Crystallogr.*, **15**, 983 (1962).
(4) D. S. Martin, *Inorg. Chim. Acta, Rev.*, **5**, 107 (1971).
(5) M. M Woolfson, "An Introduction to X-Ray Crystallography", Cambridge University Press, London, 1970, p 244.
(6) W. R. Busing, K. O. Martin, and H. A. Levy, "ORFLS, a Fortran Crystallographic Least Squares Program", USAEC Report ORNL-TM-305, Oak Ridge National Laboratory, Oak Ridge, Tenn., 1962.
(7) R. A. Doyle and P. S. Turner, *Acta Crystallogr., Sect. A*, **24**, 390 (1968).
(8) D. J. Wehe, W. R. Busing, and H. A. Levy, "ORABS, a Fortran Program for Calculating Single Crystal Absorption Corrections", USAEC Report ORNL-TM-229, Oak Ridge National Laboratory, Oak Ridge, Tenn., 1962.
(9) J. D. Scott, private communication, 1971.
(10) Supplementary material.
(11) A. Bondi, *J. Phys. Chem.*, **68**, 441 (1964).
(12) P. J. Hendra, J. *Chem. Soc. A*, 1298 (1967).
(13) P. E. Fanwick and D. S. Martin, Jr., *Inorg. Chem.*, **12**, 24 (1972).
(14) P. A. Vaughan, J. H. Sturdivant, and L. Pauling, *J. Am. Chem. Soc.*, **72**, 5477 (1950).
(15) C. K. Jorgensen, *Acta Chem. Scand.*, **10**, 518 (1956).